

U. S. DEPARTMENT OF COMMERCE
NATIONAL OCEANIC AND ATMOSPHERIC ADMINISTRATION
NATIONAL WEATHER SERVICE
NATIONAL METEOROLOGICAL CENTER

OFFICE NOTE 349

APPLICATION OF IMPLICIT NORMAL MODE INITIALIZATION
TO THE NMC NESTED GRID MODEL

DAVID F. PARRISH
DEVELOPMENT DIVISION

JANUARY 1989

THIS IS AN UNREVIEWED MANUSCRIPT, PRIMARILY INTENDED FOR
INFORMAL EXCHANGE OF INFORMATION AMONG NMC STAFF MEMBERS.

1. INTRODUCTION

Several techniques now exist for the initialization of limited area models that are good approximations to nonlinear normal mode initialization (NLNMI), but which do not require computation of normal modes (Bourke and McGregor, 1983, Juvanon du Vachet, 1986, for example). Ballish (1979) provided an early intercomparison of some non-normal mode methods with normal mode procedures using a global model. However, a complete investigation of non-normal mode schemes has recently been provided by Temperton (1988, 1989; henceforth, T88 and T89) for limited area and spectral model applications. The derivation in T88 unifies the various methods and also brings forth an "improved" scheme, which is virtually identical to current global NLNMI procedures. Normal modes are actually used in the derivations of T88, but because the actual initialization does not require explicit normal mode computations, it is appropriately referred to as "implicit normal mode initialization" (INMI).

The essential feature of INMI is that transformations between physical and normal mode space are replaced by elliptic boundary value problems which are solved in physical space. That this should be possible is not surprising. Leith (1980) demonstrated clearly the relationship between quasigeostrophic balance equations and normal mode initialization for an f-plane model. What Temperton has done is to create a variant of these equations which is energetically consistent on a sphere, while at the same

time keeping the full variability of the Coriolis parameter. The price to pay for this result is elimination of the beta term in the vorticity equation, which gives rise to Rossby wave motion. While this might seem a heavy cost, in fact, for the purpose of describing balance, the effect is negligible.

To apply INMI to the National Meteorological Center Nested Grid Model (NGM, Phillips, 1979), it is necessary to solve boundary value problems on the nested grids. Multigrid methods (Fulton et al, 1986) appear to be ideally suited because of the NGM grid nesting, but the procedures are complex and require a lot of development. An alternative approach is to embed the boundary value problem on the entire sphere and then solve it using spherical harmonics (an idea suggested by Machenhauer except that normal modes are used instead of the implicit method). This idea is easy to implement and allows for the possibility of a universal "black box" INMI, applicable to any model with little special programming.

However, this approach has two disadvantages. First, because the spectral and finite difference solutions of the boundary value problems diverge from each other significantly as the grid scale is approached, the balance achieved is not very good for small scales. Second, for high resolution models, extension to the globe is costly. In practice, the first disadvantage doesn't seem to be a problem, at least for the NGM. The second problem may be resolved by using the Schmidt (1977) sphere-to-sphere conformal map, which defines a new latitude-longitude coordinate system with locally high resolution.

The present operational initialization (Hoke et al, to appear) of the NGM is similar to the above mentioned process, but with an important difference. Initialization is done using a hemispheric spectral model with the same vertical structure as the NGM (similar to the Canadian approach, Verner and Benoit, 1984). This result is interpolated horizontally to the NGM grids. Because of this, the resolution of the model variables, and in particular, the terrain, is limited to that of the hemispheric spectral model (currently R80). The method described here uses the spectral approach only to solve the INMI boundary value problems. This generates balancing corrections which are applied directly to the model grid. Only the balance correction is constrained by resolution of the spectral representation, not the full fields. Both procedures appear to give almost identical results for the current NGM model, with perhaps a slight advantage in forecast skill going to the new INMI.

In the remainder of this paper, we have first a brief derivation of INMI (scheme B from T89). Then follows in section 3 the details of implementation for the NGM. Results, complete with obligatory barographs, are next. The concept of incremental initialization, which is used in the operational implementation of the INMI, is introduced in section 5. Some results of a parallel test are also presented. Discussion and conclusion complete this note.

2. IMPLICIT INITIALIZATION

The following is a brief presentation of INMI as carefully described in T88. The interested reader is urged to examine both

T88 and T89 for excellent treatments of the details.

The starting point for all normal mode initialization methods is an appropriate linearization of the prediction equations. Because extension in the vertical coordinate is treated identically for all schemes (a vertical mode decomposition is defined), we need consider only the shallow water equations, which are written here in vorticity-divergence form:

$$\dot{z} = B \nabla^{-2} z - F \nabla^{-2} d + r_z \quad (2.1a)$$

$$\dot{d} = F \nabla^{-2} z + B \nabla^{-2} d - g \nabla^2 h + r_d \quad (2.1b)$$

$$\dot{h} = -\bar{h} d + r_h \quad (2.1c)$$

z is the relative vorticity

d is the divergence

h is the free surface elevation

\bar{h} is the scale depth for a given vertical mode

r_z, r_d, r_h are non-linear residuals

\dot{z} is local time derivative

$$B = k^* \nabla_x (f \nabla)$$

$$F = \nabla^* (f \nabla)$$

f is the Coriolis parameter

k is the vertical unit vector

∇^{-2} symbolizes the inversion of ∇^2 under appropriate boundary conditions.

Equations (2.1) represent the standard linearization upon which global normal mode procedures are based. The implicit schemes start with various modified linear models. We will only consider scheme B from T89, which was judged to be the "best" in the sense that it is closest to the standard linear model and is energetically consistent. To get this model, we take the first term on the rhs of (2.1a) and add it to the nonlinear residual, getting,

$$\dot{z} = -F \nabla^{-2} d + r'_z \quad (2.1a')$$

Thus the linear model we will be using as the basis for initialization is:

$$\dot{z} = -F \nabla^{-2} d \quad (2.2a)$$

$$\dot{d} = F \nabla^{-2} z + B \nabla^{-2} d - g \nabla^2 h \quad (2.2b)$$

$$\dot{h} = -\bar{h}d \quad (2.2c)$$

INMI depends upon distinguishing the fast and slow parts of a state without resorting directly to using normal modes. To see how this can be done with the modified linear model (2.2), we first suppose that any variable has a slow and a fast part, viz.

$$z = z_s + z_f$$

where s and f refer to slow and fast. The slow modes are non-divergent for the modified linear model. Using this knowledge and the orthogonality of all slow modes to all fast modes, equations (2.2) reduce to the following relationships for the slow and fast components of a given state:

$$\dot{z}_s = 0 \quad (2.3a)$$

$$\dot{z}_f = -F \nabla_f^{-2} d_f \quad (2.3b)$$

$$0 = F \nabla_s^{-2} z_s - g \nabla_s^2 h_s \quad (2.3c)$$

$$\dot{d}_f = F \nabla_f^{-2} z_f + B \nabla_f^{-2} d_f - g \nabla_f^2 h_f \quad (2.3d)$$

$$\dot{h}_s = 0 \quad (2.3e)$$

$$\dot{h}_f = -\bar{h} d_f \quad (2.3f)$$

From (2.3a,e) we see that the slow modes for this linear model are stationary as well as non-divergent. Equation (2.3c) is a form of the linear balance equation which provides a relationship between z_s and h_s . A similar relationship can be obtained for z_f and h_f by eliminating d_f between (2.3f) and (2.3b), integrating in time, and noting that the integration constant must be zero (see T88 for proof). There results

$$z_f = \bar{h}^{-1} F \nabla_f^{-2} h_f \quad (2.4)$$

Relationships (2.3) and (2.4) allow decomposition of a state (z,d,h) into its slow and fast parts. The following procedure illustrates one way to do this:

$$(1) \text{ define and calculate } w_f = F \nabla_f^{-2} z_f - g \nabla_f^2 h_f$$

(w_f contains only fast modes because of (2.3c))

(2) (a) observe that because of (2.3c)

$$F \nabla_f^{-2} z_f - g \nabla_f^2 h_f = w_f$$

(b) substitute for z_f using (2.4) to get

$$[(g\bar{h})^{-1} (F \nabla_f^{-2})^2 - \nabla_f^2] h_f = g^{-1} w_f$$

(c) solve for h_f

(3) compute z_f from (2.4), $z_f = \bar{h}^{-1} F \nabla_f^{-2} h_f$

(4) $z_s = z - z_f$; $d_s = 0$; $d_f = d$; $h_s = h - h_f$

By purely algebraic manipulation in physical space it is possible to find slow and fast parts of a state. When solving for h_s , and when wind components are obtained from vorticity and divergence, care must be given to the boundary conditions used. See T88 for a very good treatment of the boundary condition problem.

Before moving on to initialization, let us first briefly review how NLNMI is usually implemented. Let

$$\dot{x} = icx + r(x)$$

represent the equation for a single gravity mode of frequency c . The Machenhauer condition (Machenhauer, 1977) is to find x , the amplitude of the gravity mode, such that the gravity mode time tendency \dot{x} is zero,

$$\dot{x} = 0.$$

We must then solve the nonlinear equation

$$icx + r(x) = 0$$

for x . Traditionally this is solved by a simple iteration. Let

$$x(n+1) = x(n) + dx(n)$$

be the result of the n-th iteration. Then we have

$$\dot{x}(n) = icx(n) + r(n) \quad (2.5)$$

$$0 = ic(x(n) + dx(n)) + r(n) \quad (2.6)$$

Solving (2.6) for $dx(n)$ and using (2.5), we see that

$$icdx(n) = -\dot{x}(n) \quad (2.7)$$

or

$$dx(n) = ic^{-1} \dot{x}(n) \quad (2.8)$$

This form is used because it is easier to compute \dot{x} than r (simply advance the model one timestep, difference and divide by dt).

This is now applied to equations (2.1). Note that "icx" is to be replaced by the rhs of (2.2). The first step is to filter slow modes out of the tendencies. In a manner similiar to before, form

$$\dot{w}_f = F \nabla_f^{-2} \dot{z} - g \nabla_f^2 \dot{h} \quad (2.9)$$

where again because of (2.3c) \dot{w}_f contains only fast components. Equation (2.9) is equivalent to

$$F \nabla_f^{-2} \dot{z}_f - g \nabla_f^2 \dot{h}_f = \dot{w}_f \quad (2.10)$$

Repeating the form of (2.7), replace \dot{z}_f and \dot{h}_f with the appropriate rhs from (2.2), and put increments dz , dd , dh in place of \dot{z} , \dot{d} , \dot{h} . There results

$$[(g\bar{h})^{-1} (F \nabla_f^{-2})^2 - \nabla_f^2] dd_f = -(g\bar{h})^{-1} \dot{w}_f \quad (2.11)$$

Equation (2.11) can be solved for the incremental change to the divergence, dd_f .

To get the remaining corrections, dz_f , dh_f , we use (2.3d) with the rhs variables again replaced by their increments. We have

$$\dot{d}_f = F \nabla_f^{-2} dz_f + \nabla_f^{-2} dd_f - g \nabla_f^2 dh_f \quad (2.12)$$

Using (2.4) ($dz_f = \bar{h}^{-1} F \nabla_f^{-2} dh_f$) again and moving the term with dd_f to the other side (since we know dd_f now), we discover that dh_f is the solution of

$$[(g\bar{h})^{-1} (F \nabla_f^{-2})^2 - \nabla_f^2] dh_f = g^{-1} (\dot{d}_f - B \nabla_f^{-2} dd_f) \quad (2.13)$$

Now that we have dh_f , we use (2.4) to get dz_f . All fast mode corrections, dz_f , dd_f , and dh_f are now available to be added directly to z , d , and h .

To summarize, one iteration of INMI, as indicated schematically by (2.8), consists of the following steps:

- (1) Execute one model timestep to get \dot{z} , \dot{d} , \dot{h} .
- (2) Compute \dot{w}_f using (2.9).
- (3) Solve (2.11) for dd_f .
- (4) Solve (2.13) for dh_f .
- (5) Use (2.4) to get dz_f .
- (6) Update z , d , h $z = z + dz_f$, etc.

As demonstrated in T89, this procedure, when done on a sphere, is identical to initialization using normal modes if the modes are obtained from the modified linear model (2.2).

3. APPLICATION TO NGM

Implicit initialization requires the solution of elliptic boundary value problems, where the elliptic operator is

$$(\bar{gh})^{-1} (F \nabla^{-2})^2 - \nabla^2$$

The correct boundary conditions are derived in T88. The solution of this elliptic problem with the appropriate bc's for the NGM is greatly complicated due to the grid nesting and the hemispheric wall condition which runs through the interior of the A-grid in a complex way. Multigrid methods can probably be used for this case, but here an approximate solution is used.

All that is required of the NGM model is variable tendencies which can easily be obtained by running the model for one time-step. To get the incremental initialization correction, we interpolate these tendencies to a Gaussian latitude-longitude grid, transform to hemispheric spherical harmonics, and then solve the elliptic problem in spectral space, where it reduces to a tridiagonal matrix. The spectral formulation is exactly as presented in T89. The resulting corrections are reconstructed on the Gaussian grid, and then interpolated to the NGM grids. This process creates a balance correction that is relatively smooth compared to the grid resolution (especially on the high-resolution C-grid). In addition, the linear model is now spectral and not directly consistent with the finite differences of the NGM. However, judging from the results, these do not appear to be limitations.

While this approach may seem cumbersome, it is actually much more straightforward than a multigrid solution. The same proce-

dure could be applied to other regional models, and in fact this was originally proposed by Machenhauer as a method for limited area initialization. The problem before, when normal modes were used, was that the initialization increments are obtained over a global domain which should have a resolution comparable to the regional model. A great deal of storage is required for the normal modes. Since the present approach does not use normal modes directly, that is no longer a problem.

Another problem, though, is that for very high resolution models, computation of increments on a global domain is too expensive (which is why the model is regional in the first place). As mentioned in the introduction, this may be addressed by solving the elliptic problem on a Schmidt coordinate. Here, we still have a latitude-longitude spherical system, and can use spherical harmonics, but now on a mapped sphere, which is rotated and stretched relative to the earth coordinates, so that a local area is emphasized. The matrix problem to solve is now block-tridiagonal and could be solved directly for moderate resolution. Solution by conjugate gradients may be preferable.

A subroutine is being developed which uses this coordinate system and will provide an initialization correction for any model given that model's tendencies and a few other descriptive items. This will initialize most models without having to design a program specifically for each one.

4. RESULTS

Here we show some results from a series of experiments. First, we have a forecast from an uninitialized analysis, then

one from the operational initialization, and finally the test initialization. The operational initialization is first-order Baer-Tribbia for two vertical modes with a hemispheric R80 spectral model using the NGM vertical structure. The initialized fields are reconstructed on a 320 x 90 Gaussian grid and interpolated horizontally to the NGM grids. The test initialization also is done for two vertical modes, but uses two iterations of solving for the Machenhauer condition that gravity tendencies be zero. The spectral truncation for solving the elliptic problems is T59. (More resolution than this appears to be unnecessary and may actually degrade the result, because of the incompatibility between the spectral and finite difference approximations.)

Figure 1 shows the surface pressure at Washington, D.C. for the three cases. The operational and test forecasts are virtually identical, and both have successfully filtered most of the large amplitude oscillations evident in the uninitialized run. The variability which remains is partly a result of initializing only two vertical modes, and partly the incompatibility between spectral and finite difference representations. Some rapid variation is also to be expected which is meteorologically correct. The high resolution part of the NGM is capable of generating rapid pressure variation in response to frontal passage and squall-line generation.

The quantity BAL, as defined in T88, is shown in figures 2 and 3 for the two vertical modes which are initialized. BAL is a measure of the energy partition between slow and fast parts of the tendencies of the model variables. Here, BAL is averaged over two-dimensional or total wave-number ranges (which are homoge-

neous, isotropic measures of scale on a sphere). First, observe that just one slow mode curve appears on each graph, since the slow mode tendencies are constant for all three experiments. This is to be expected, because only the fast modes are altered by both the operational and test initializations. Second, notice that the tendency of fast modes for each iteration of the test initialization is reduced much more for large scales. Convergence is slow for the smallest scales being initialized. This is probably caused by the incompatibility between the spectral representation used to generate initialization corrections and the NGM finite differences used to compute the tendencies.

A comparison of the operational fast mode tendency amplitude against two iterations of the test scheme show that they are similar, with the test result "better" for larger scales and the operational slightly "better" for smaller scales. "Better" is used in quotes here because, as pointed out by Phillips (1981), the fast mode tendencies should not be zero as the Machenhauer condition requires, but instead should have amplitude comparable to the slow mode tendencies. By this measure, the operational and test schemes are in approximate agreement, since the fast mode tendencies are comparable or less than the slow mode values for all scales represented here.

Because the INMI computes initialization corrections with a T59 spectral representation, the difference between analyzed and initialized fields is smoother relative to the operational result, which is R80. This can be seen in figures 4 and 5, which depict changes in the 500mb heights due to initialization for the test and operational schemes respectively. Apart from the

smoother result for the INMI, the two systems produce approximately the same adjustments. 48 hour forecasts from each of these initial conditions produce virtually identical results, as can be seen in figures 6 and 7, which show differences of each with the verifying operational analysis. For reference, the operational analysis valid at each time is presented in figures 8 and 9.

5. INCREMENTAL INITIALIZATION

By incremental initialization, we mean that initialization is applied only to an analysis increment, leaving the first guess to the analysis unchanged. A persistent problem with NLNMI is that many physical processes in the model (particularly convection) are incorrectly initialized--the initialized divergence amplitude is significantly underestimated. By modifying just the analysis increment, the divergent response to model physics remains intact. Thus, the initialization can be adiabatic, with diabatic processes passed on implicitly in the forecast first guess. If data assimilation is done with an interval of 6 hours or less, this may be a good approximation.

To understand incremental initialization, we go back to the simple representation for a single normal mode of frequency c :

$$\dot{x} = icx + r(x) \quad (5.1)$$

Let x_b represent the first guess field, and x_a the analysis. Each field separately satisfies an equation of the form (5.1):

$$\dot{x}_b = icx_b + r_b \quad (5.2)$$

$$\dot{x}_a = icx_a + r_a \quad (5.3)$$

Now, under the basic assumption

that \dot{x}_b is in desirable balance and is not to be altered, subtract (5.2) from (5.3) to get a non-linear increment equation

$$\dot{y} = ic_y + s \quad (5.4)$$

where $y = x_a - x_b$ and $s = r_a - r_b$.

Equation (5.4) has the same form as (5.1) and we can write immediately the same result as in section 2. One iteration of non-linear incremental initialization is described by

$$dy(n) = ic^{-1} y(n)$$

Notice that dy can be added directly to x --the difference field y is not required in the computation. We have

$$x(n+1) = x(n) + dy(n).$$

Incremental initialization can be implemented with only a minor change to the standard NLNMI scheme. We first compute once and save the tendencies of the first guess, x_b . Then for each iteration of NLNMI, we first compute \dot{x} in the usual way, but then subtract \dot{x}_b to get the desired increment equation tendency. The rest is as before.

6. RESULTS FROM A PARALLEL TEST

The initialization of increments, described in the last section, is difficult to test in isolation. However, it is an integral part of the proposed replacement for the operational NGM initialization, which was compared to the operational system in a parallel test. The test system contains several steps. First, the first guess from the spectral model is interpolated vertically and horizontally to the NGM grids. A full field INMI is

applied at this point to remove imbalances introduced because of the vertical interpolation. (This was suggested by work of Lorenc, 1988. He found that initialization changes were larger than analysis corrections and seemed to result from the vertical interpolation and corresponding change of model terrain.) Next, analysis increments are obtained and added on to these initialized first guess fields on the NGM model grids. Finally, an incremental INMI is applied to this result, using as a reference, the initialized first guess.

The parallel test experiment was conducted over the period of 28 June 0000GMT to 8 July 1200GMT, 1988. The results show that the two systems are very close, with perhaps a slight advantage going to the test system. Figure 10 shows the surface pressure for the two systems at Oklahoma City. There is a pulse with amplitude of about 2mb at 18 hours in the operational system which is absent in the test run. This probably comes from the Himalayan plateau. Otherwise, the two traces agree very well. The rms sigma-dot values shown in the figure are consistently slightly smaller for the test run, also indicating a slight improvement in balance.

7. CONCLUSION

The results presented in this paper demonstrate that implicit normal mode initialization can be successfully applied to a model with nested grids and complex boundary conditions. The application is approximate, however, since a spectral technique is used to solve the elliptic boundary value problems which are a part of INMI. For this reason, small scales are not well bal-

anced by this procedure. This is not considered to be a problem, at least for the NGM model, for two reasons. First, the Lax-Wendroff time differencing scheme very quickly eliminates oscillations which result from 4-grid increment and smaller gravity waves. Second, the model parameterizations continually introduce small scale noise, which is controlled by the time-differencing and some spatial smoothing.

Direct solution of the "correct" (ie finite difference) elliptic problems using consistent model discretization seems desirable and gives the best balance, as T88 results demonstrate. However, it may be quite difficult to set up and solve the appropriate elliptic problem for some models, as is the case for the NGM which has nested grids and complicated boundary conditions. The alternative approach used here of imbedding the problem on a sphere and solving with spherical harmonics, appears to produce an adequate result and should be applicable in "black box" form to any model with little special formulation required. The principle limitation of this method is the requirement of high resolution over the entire globe for application to high resolution limited area models, which is computationally wasteful. As pointed out earlier, the Schmidt variable resolution sphere-to-sphere mapping might provide a reasonable solution. Work is currently in progress on a "black box" initialization algorithm which incorporates the variable resolution map.

The idea of incremental normal mode initialization was also presented. Initialization, when applied to full fields, can be very disruptive of divergent motions that exist in response to convective activity. At NMC, we currently initialize only 2

vertical modes as a partial solution to this problem (Carr et al, 1988). By applying the initialization adjustment only to the analysis increment, a further improvement in the short-range forecast behavior can be realized. While our use of the incremental procedure is primarily intended for the NGM in an experimental high-resolution data-assimilation system, it is also used in the operational NGM initialization to reduce the effect of interpolation error in the NGM analysis.

Incremental INMI, as described here, was implemented into the operational regional analysis and forecast system (RAFS) at NMC in December of 1988.

REFERENCES:

- Ballish, B., 1979: Comparison of some nonlinear initialization techniques. Preprints Fourth Conf. on Numerical Weather Prediction, Silver Spring, Amer. Meteor. Soc., 9-12.
- Bourke, W., and J.L. McGregor, 1983: A nonlinear vertical mode initialization scheme for a limited area prediction model. Mon. Wea. Rev., 111, 2285-2297.
- Carr, F.H., R.L. Wobus, and R.A. Petersen, 1988: Initialization experiments with the NMC nested grid model. Preprints, Eighth Conf. on Numerical Weather Prediction, Baltimore, MD, 22-26 Feb. 1988, 758-765.
- Fulton, S.R., P.E. Ciesielsky, and W.H. Schubert, 1986: Multigrid methods for elliptic problems: a review. Mon. Wea. Rev., 114, 943-959.
- Hoke, J.E., N.A. Phillips, G.J. DiMego, J.J. Tuccillo, and J.G. Sela, 1989: The regional analysis and forecast system of the National Meteorological Center. submitted to Weather and Forecasting.
- Juvanon du Vachat, R., 1986: A general formulation of normal modes for limited-area models: applications to initialization. Mon. Wea. Rev., 114, 2478-2487.
- Leith, C.E., 1980: Nonlinear normal mode initialization and quasigeostrophic theory. J. Atmos. Sci., 37, 958-968.
- Lorenc, A.C., 1988: A practical approximation to optimal four-dimensional objective analysis. Mon. Wea. Rev., 116, 730-745.

- Machenhauer, B., 1977: On the dynamics of gravity oscillations in a shallow water model, with application to normal mode initialization. Contrib. Atmos. Phys., 50, 253-271.
- Phillips, N., 1979: The Nested Grid Model. NOAA Technical Report NWS 22, Dept. of Commerce, Silver Spring, Maryland, 80 pp.
- Phillips, N., 1981: Treatment of normal and abnormal modes. Mon. Wea. Rev., 109, 1117-1119.
- Schmidt, F., 1977: Variable fine mesh in a spectral global model. Contrib. Atmos. Phys., 50, 211-217.
- Temperton, C., 1988: Implicit normal mode initialization. Mon. Wea. Rev., 116, 1013-1031.
- Temperton, C., 19???: Implicit normal mode initialization for spectral models. Submitted for publication in Mon. Wea. Rev.
- Verner, G., and R. Benoit, 1984: Normal mode initialization of the RPN finite element model. Mon. Wea. Rev., 112, 1535-1543.

Figure captions

- Fig. 1. Surface pressure at Washington, DC. Solid line with pluses is no initialization. Dotted line with triangles is operational initialization. Dashed line with circles is test initialization.
- Fig. 2. The quantity BAL (mean square of tendency amplitude in energy units). Ordinate is $\log_{10}(\text{BAL})$. Abscissa is two-dimensional or total wave number groups. The solid line with pluses represents the slow mode mean square tendency. The corresponding fast mode quantities are shown for iterations 0, 1 and 2 (short dash, long dash, and dots). Fast mode tendency after operational initialization is represented with the dot-dash. All for vertical mode 1.
- Fig. 3. Same as Fig. 2 but for vertical mode 2.
- Fig. 4. Change to 500mb heights caused by INMI.
- Fig. 5. Same as Fig. 4 for operational initialization.
- Fig. 6. 48hr forecast of 500mb height (INMI - no init).
- Fig. 7. Same as Fig. 6 for operational initialization.
- Fig. 8. Initial 500mb height after operational initialization.
- Fig. 9. Operational 48hr forecast of 500mb height.
- Fig. 10. RMS sigma-dot and surface pressure variations at 5 minute intervals for operational and parallel systems. (Parallel system contains INMI to be implemented.)

SURFACE PRESSURE TRACE

—+— no init -Δ- oper init -○- test init

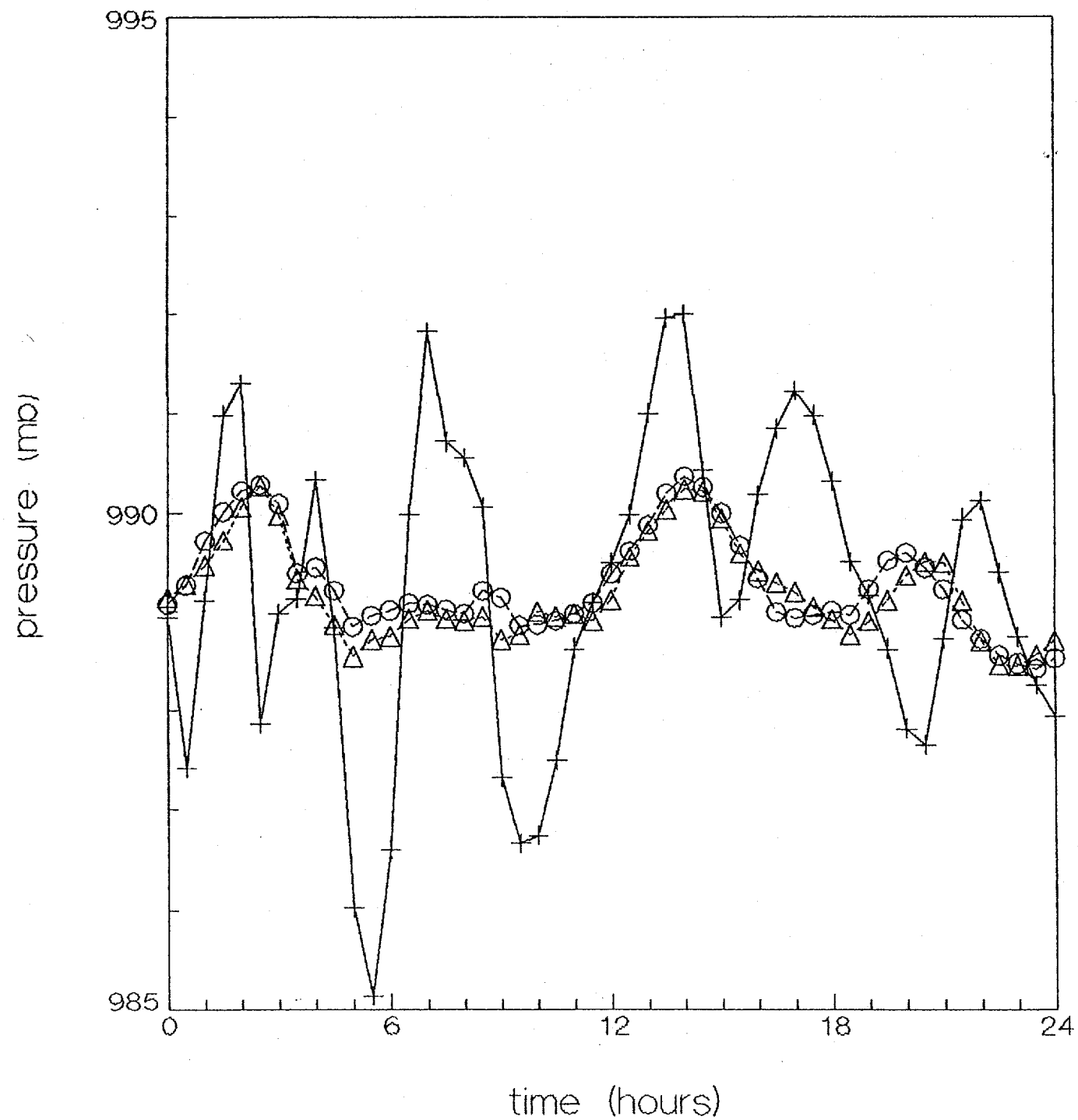


Fig. 1

BALANCE STATISTICS FOR INITIALIZATION vertical mode 1

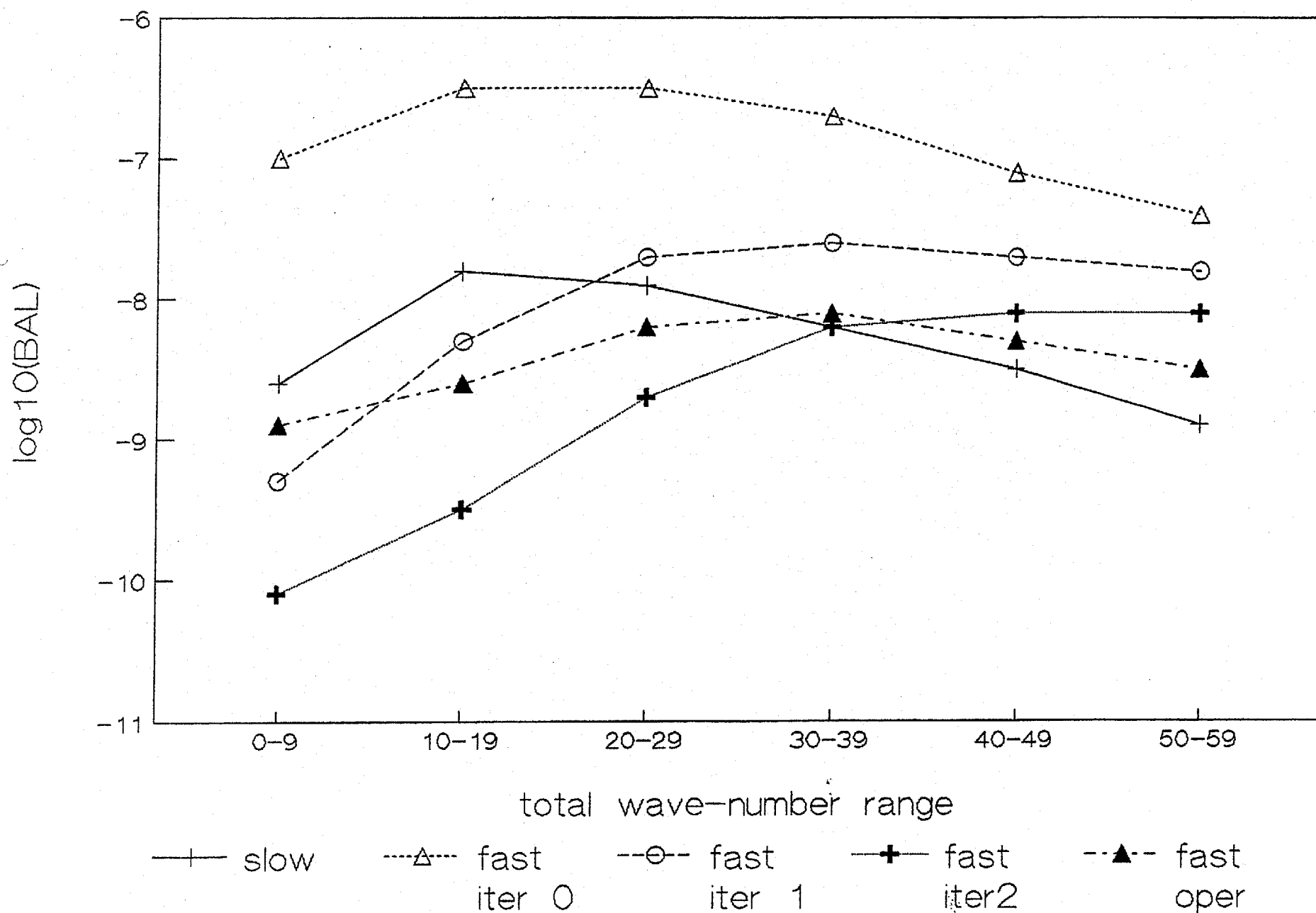
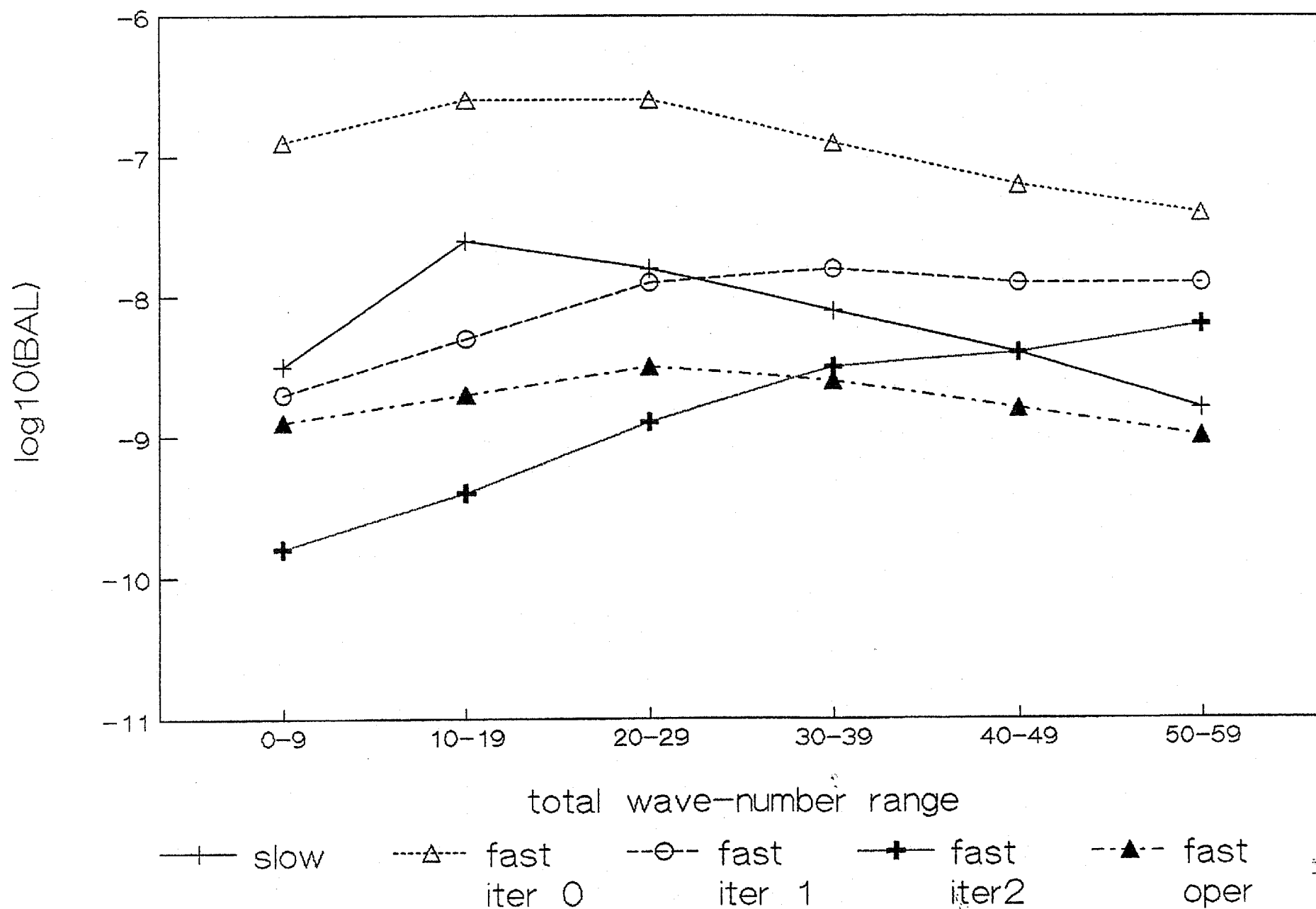
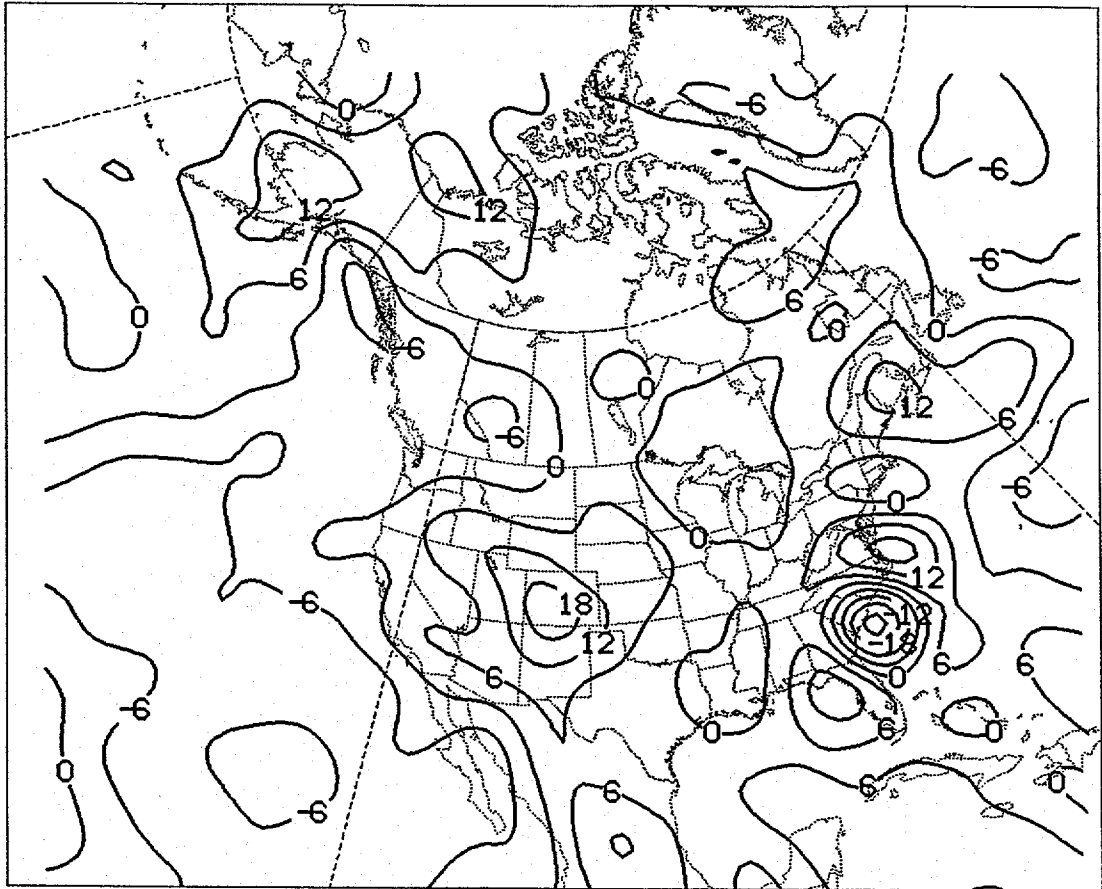


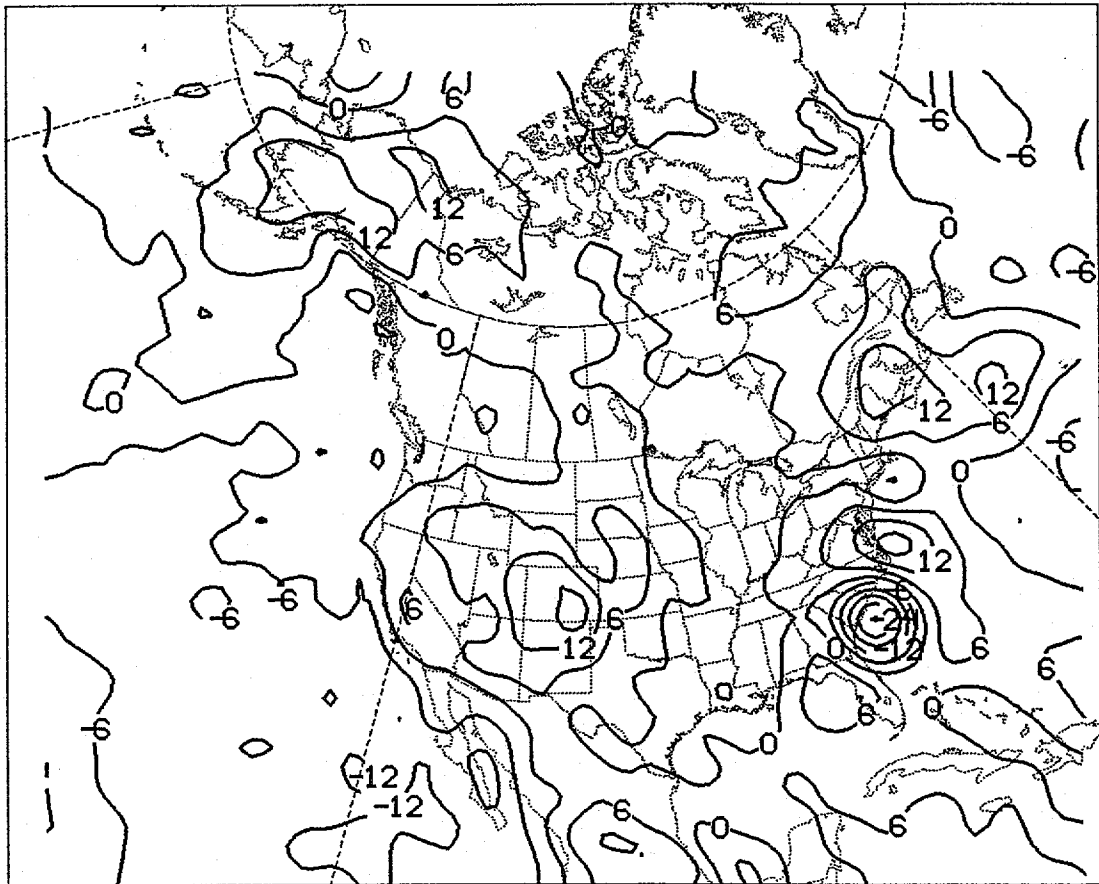
Fig. 2

BALANCE STATISTICS FOR INITIALIZATION vertical mode 2

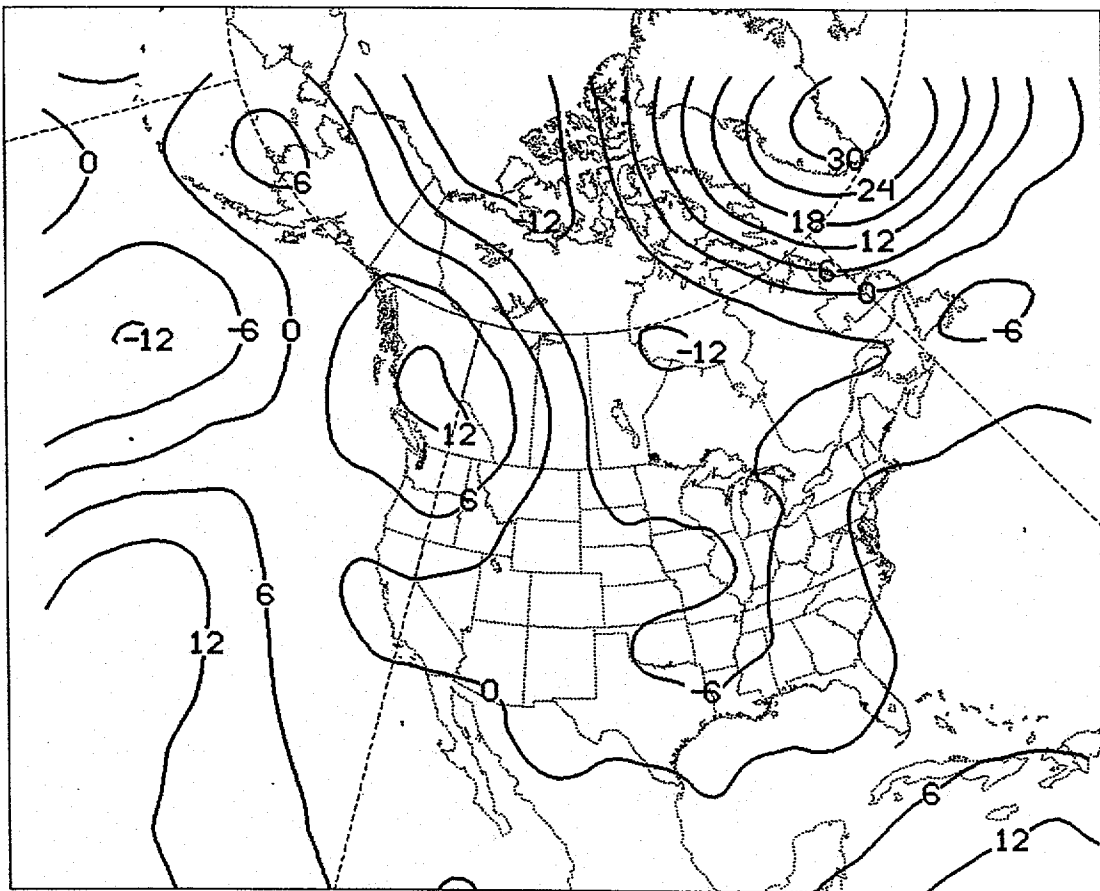




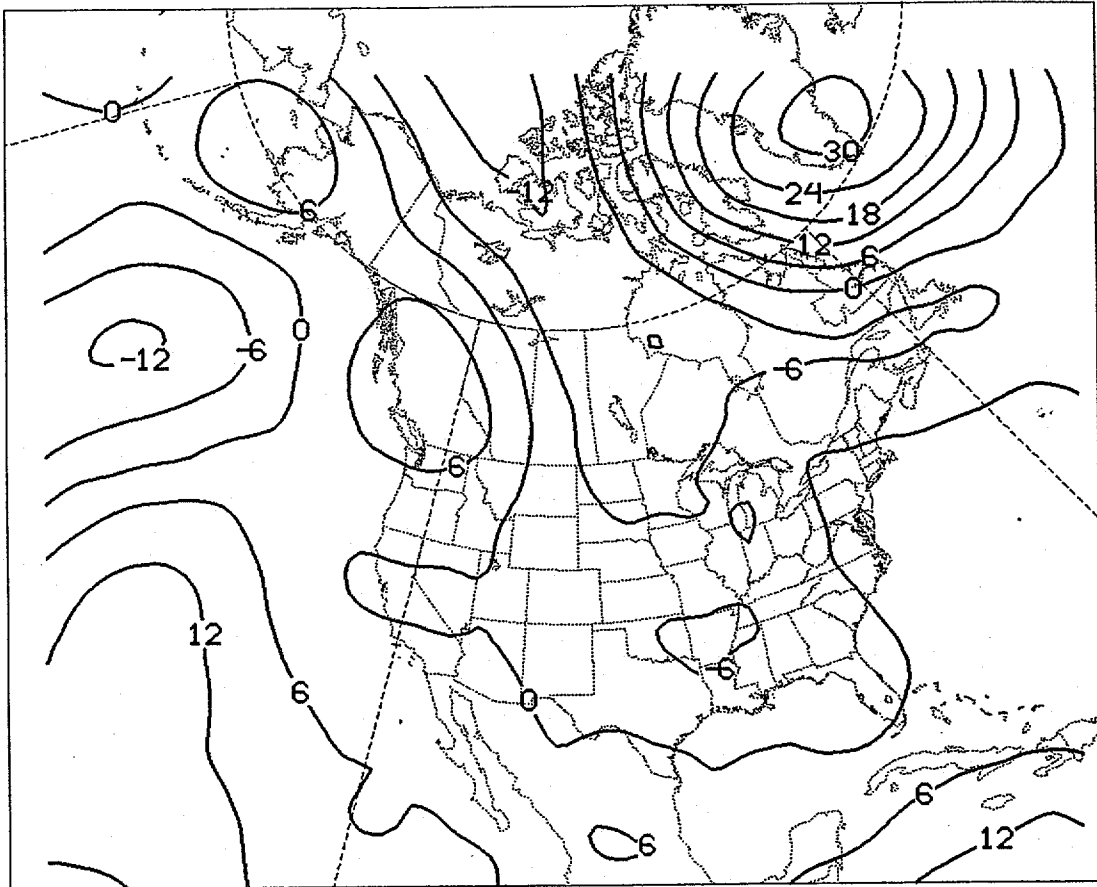
500MB HEIGHT (M)
VALID FOR 00Z 11 MAR 88
IMPLICIT - NO INI



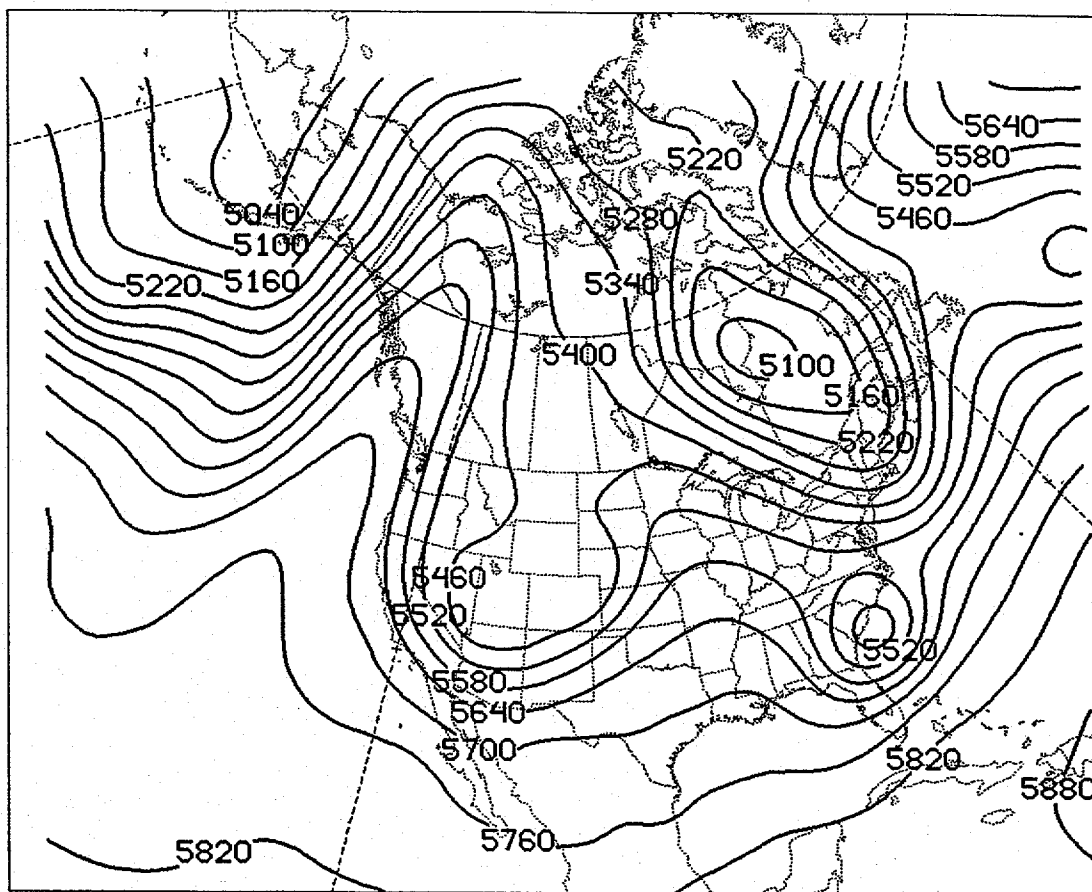
500MB HEIGHT (M)
VALID FOR 00Z 11 MAR 88
SPECTRAL - NO INI



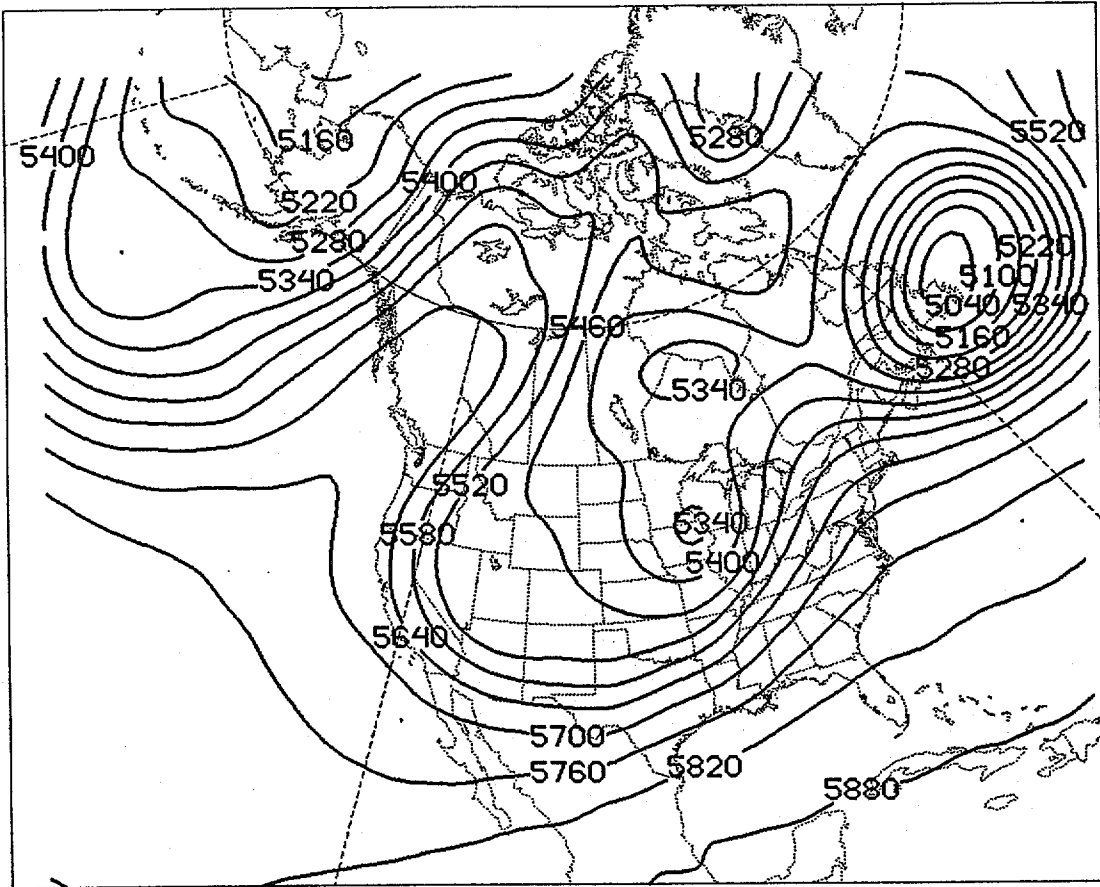
500MB HEIGHT (M)
48 HOUR FORECAST
IMPLICIT - NO INI



500MB HEIGHT (M)
48 HOUR FORECAST
SPECTRAL - NO INI



500MB HEIGHT (M)
VALID FOR 00Z 11 MAR 88
SPECTRAL



500MB HEIGHT (M)
48 HOUR FORECAST
SPECTRAL

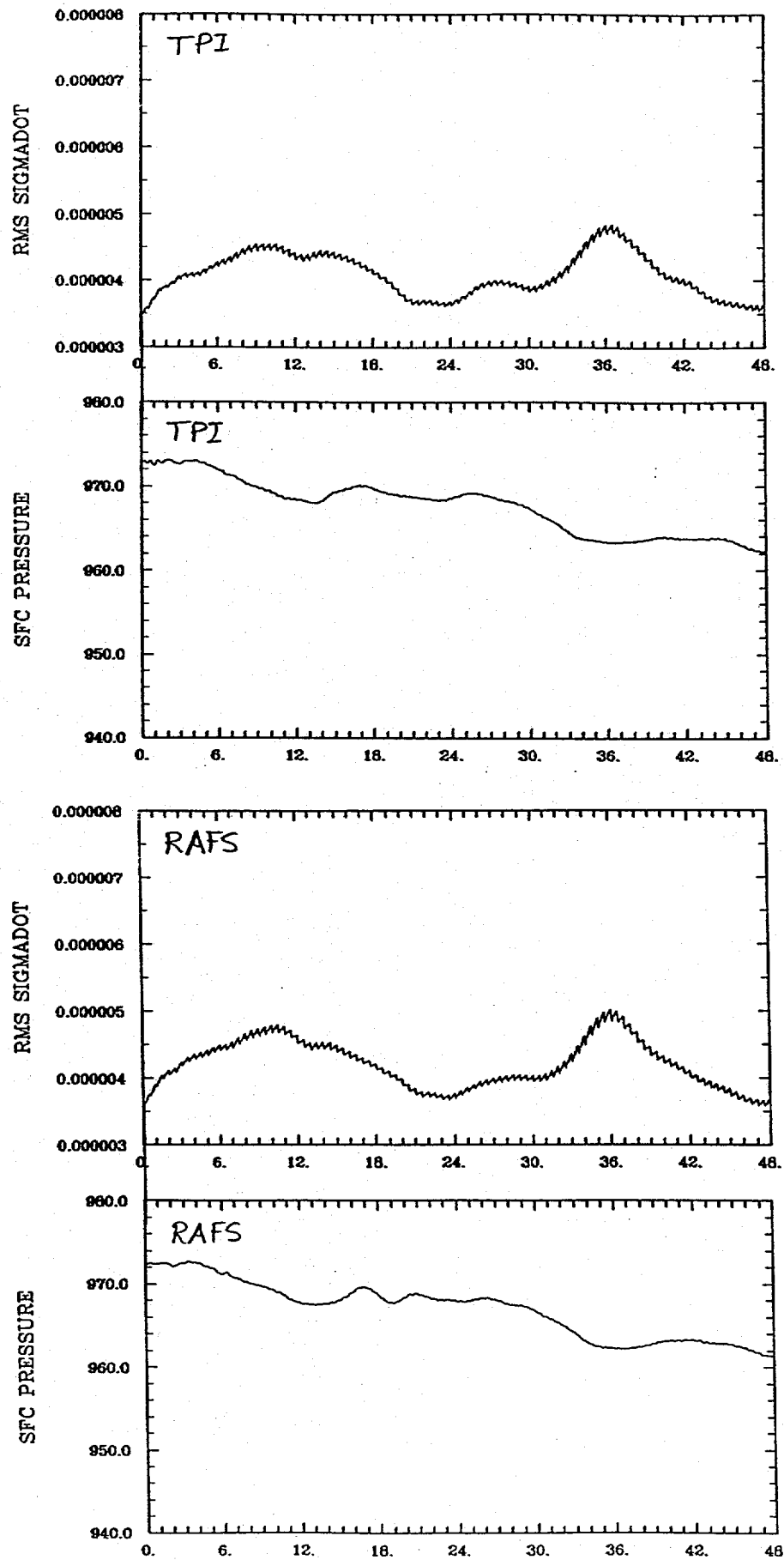


Fig. 10